Glycogen Metabolism in Aerobic Mixed Cultures

K. Dircks,[1] J. J. Beun,[2] M. van Loosdrecht,[2] J. J. Heijnen,[2] M. Henze[1]

[1]Department of Environmental Science and Engineering, Technical University of Denmark, Lyngby, Denmark; telephone: +45-4525-1477; fax: +45-4593-2850; e-mail: mh@imt.dtu.dk
[2]Kluyver Laboratory for Biotechnology, Delft University of Technology, Julianalaan 67, 2628 BC Delft, The Netherlands

Received 15 April 2000; accepted 24 October 2000

Abstract: In this study, the metabolism of glycogen storage and consumption in mixed cultures under aerobic conditions is described. The experimental results are used to calibrate a metabolic model, which as sole stoichiometric variables has the efficiency of oxidative phosphorylation (δ) and maintenance requirement in units of adenosine triphosphate (m_{ATP}). Using the experimental data and values from the literature we show that δ and m_{ATP} are strongly coupled and that the values determined for glycogen and poly-β-hydroxybutyrate (PHB) metabolism are similar. We also demonstrate that storage of glycogen and subsequent growth occur without significant loss of energy, as compared with direct growth on glucose. For kinetic modeling, Monod kinetics is used most commonly in activated sludge models to describe the rate of microbial transformation. Monod kinetics, however, does not provide a good description of the data obtained. Second-order kinetics gives a better description of the rate of glycogen degradation. Formation and consumption of glycogen appears to be much faster than for PHB. © 2001 John Wiley & Sons, Inc. *Biotechnol Bioeng* **73**: 85–94, 2001.
Keywords: activated sludge; aerobic; feast–famine regime; glucose; glycogen; mathematical model; storage; yield coefficient

INTRODUCTION

Based on the literature, there is the general belief that, under conditions in which microbial growth is limited by some factor other than carbon and energy source, accumulation of reserve material is most likely to occur (Dawes and Senior, 1973). This belief originated from a large number of observations pertaining to the ability of bacteria to store substrate (e.g., Wilkinson, 1959). Recognition of this ability to store organic matter has lead to a new theory for the bacterial selection mechanisms in wastewater treatment processes: The dynamic substrate conditions found in wastewater treatment plants lead to a situation in which bacteria capable of storing substrate are the fittest for survival. This is based on the assumption that the stored material will allow the bacteria to obtain a more balanced growth when living under both feast and famine conditions. Bacteria capable of storage and of using this to obtain more balanced growth will be selected as opposed to those that are simply growing as rapidly as possible when substrate is present and decaying when no substrate is present (Van Loosdrecht et al., 1997). The important role of storage polymers in activated sludge processes has been recognized in experiments (Cech and Chudoba, 1983; Dircks et al., 1999; Goel et al., 1998; Krishna and Van Loosdrecht, 1999) and in modeling (Gujer et al., 1999).

Organic storage polymers are, in general, divided into two major groups of compounds: polysaccharides and lipids (including polyhydroxyalkonates) (Dawes and Senior, 1973). The different storage polymers originate from different metabolites. Glycogen is formed when the primary substrate is glucose or a compound that can be converted into pyruvate with an increase in reducing power; for example, different carbohydrates, glycerol, or proteins. Poly-β-hydroxybutyrate (PHB) is formed from substrates converted to acetyl-coenzyme A (acetyl-CoA; Stainer et al., 1959). The stoichiometry and kinetics of PHB metabolism have been described by Beun et al. (2000a). By performing similar experiments with glucose instead of acetate as the single energy source, one can compare the metabolism of glycogen to that of PHB. The aim of the present study is to describe the metabolism of glycogen in activated sludge, and to compare it with that of PHB. This is of great interest for the design, operation, and modeling of real wastewater treatment plants. In the recently published activated sludge model (ASM3) (Gujer et al., 1999), it is, as a simplification, initially assumed that all substrates are stored and that growth occurs merely on the stored substrates. Krishna and Van Loosdrecht (1999) concluded that the assumption of storage followed by growth in ASM3 could reasonably describe the experimental data obtained, but stated that if growth in the feast phase is included in the ASM3, a more consistent description could be provided.

MATERIALS AND METHODS

Experimental Set-Up

The study was performed in a 2-L double-jacketed laboratory fermentor equipped with pH and O_2 electrodes. The

Correspondence to: M. Henze

© 2001 John Wiley & Sons, Inc.

reactor was operated as a sequencing batch reactor (SBR) with a cycle length of 4 h and each cycle consisting of six process operation phases (Table I).

The pH was maintained at 7 ± 0.05 using 1 *M* HCl or 1 *M* NaOH. The stirrer speed was 300 rpm, except for the settling period and effluent withdrawal. Airflow of 1 Nl/min (SRT 3.7 days) and 1.6 Nl/min (SRT 7.7 days) was maintained, except for the period during which excess sludge was discharged and for the period of settling and effluent withdrawal. The temperature was kept at 20°C by circulating water from a thermostat water bath around the reactor.

The performance of the reactor was monitored by a bioprocessor connected on-line to the BIODACS data acquisition and control program (Applikon Schiedam, The Netherlands). To prevent the possible influence of nitrification on the measurements, allylthiourea (ATU) was regularly added to the reactor to a concentration of 100 mg/L. An inoculum activated sludge from a nitrogen-removing municipal wastewater treatment plant situated in the city of Rotterdam, The Netherlands, was used.

In cycle measurements, the substrate dosage technique was changed from pumping over a 3-min period to an instantaneous dosage with a syringe due to the fast uptake of the dosed glucose.

Substrate

Synthetic wastewater containing glucose 2.08 m*M* glucose (400 mg COD/L), NH_4Cl 2.00 m*M*, KH_2PO_4 1.65 m*M*, $MgSO_4 \cdot 7H_2O$ 0.37 m*M*, KCl 0.50 m*M*, and 1 mL/L trace element solution (Vishniac and Santer, 1975) was added to the reactor in each cycle.

Analysis

The dissolved oxygen (DO) concentration and the pH in the reactor were measured on-line with electrodes. The CO_2 content in the incoming air and in the off-gas was measured on-line with an infrared CO_2 analyzer. Samples were filtered over 0.45-μm membrane filters. The NH_4^+ concentration was measured spectrophotometrically at 630 nm with an autoanalyzer (Model 5010, Skalar). TOC was measured on a TOC analyzer (Model TOC-5050A, Shimadzu). PHB content was determined according to Beun et al. (2000b). Glycogen was determined following the method described by Smolders et al. (1994), with the modification that the time for heating at 100°C was prolonged from 1 to 5 h. The content of ash of the biomass was determined according to Dutch Standard Method NEN6621 (NNI, 1982). The elemental composition (elements C, H, N, S) of the biomass was measured by flash combustion in a partial oxygen atmosphere at 1020°C using a Carlo-Erba elemental analyzer (Model EA1108). The oxygen content of the biomass was calculated by subtracting the percentages of C, H, N, S, and ash from 100%.

CALCULATION PROCEDURE

The biomass concentration in the reactor was calculated by:

$$TOC_{biomass} = (TOC_{total} - TOC_{filtered}) \quad [C\text{-mmol/L}] \qquad (1)$$

The true SRT in the reactor was determined as:

$$SRT = \frac{\text{Amount of } TOC_{biomass} \text{ in the reactor}}{\text{Amount of } TOC_{biomass} \text{ in the effluent and waste sludge removed per day}} [\text{days}] \qquad (2)$$

The active biomass (C_X) was calculated as:

$$C_X = TOC_{biomass} - glycogen_{end\ of\ famine} \quad [C\text{-mmol/L}] \qquad (3)$$

The active biomass concentration was assumed to be constant during one cycle of the SBR (maximum change 4%).

The fraction of glycogen of the active biomass (f_{gly}) was calculated as the amount of glycogen measured (C-mol/L) divided by the amount of active biomass present in the reactor (C-mol/L), calculated using Eq. (3).

The parameter estimation was done using the computer program AQUASIM (Reichert et al., 1998).

The period during which there is soluble glucose present in the reactor is considered the feast phase. The remainder of the cycle is considered the famine phase.

METABOLIC MODEL

The metabolic model describes the aerobic metabolism of a bacterium, where growth occurs on the primary substrate, glucose, or the secondary substrate, stored glycogen. In both cases ammonium is the N source. The model consists of six internal reactions as shown in Figure 1.

Table I. Different phases in the reactor cycle.

Description	Duration (min)	Time (min)	Aeration	Stirrer
Sludge is stirred and aerated, $V = 1$ L	10	0–10	on	on
Addition of influent, 1 L	3	10–13	on	on
Aeration	207	13–220	on	on
Withdrawal of surplus sludge	2	220–222	off	on
Settling phase	15	222–237	off	off
Effluent discharge to $V = 1$ L	3	237–240	off	off

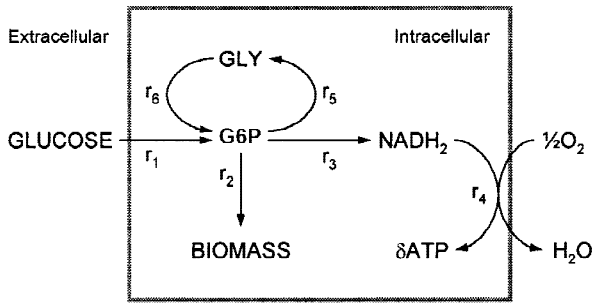

Figure 1. The structure of the metabolic model with its six internal reactions. G6P, glucose-6-phosphate; GLY, glycogen.

Reaction 1: Synthesis of Glucose-6-Phosphate from Glucose

$$-CH_2O - \frac{1}{6}\,ATP + \mathbf{G6P} = 0 \qquad (R1)$$

Adenosine triphosphate (ATP) is used to phosphorylate glucose into glucose-6-phosphate (G6P; elemental composition CH_2O in the model) during uptake (Stouthamer, 1973).

Reaction 2: Synthesis of Biomass from G6P

The synthesis of new biomass is described by Reaction (2):

$$-(1+\varepsilon_x)\mathbf{G6P} - zNH_3 - \left(\alpha_m + \alpha_x + \frac{m_{ATP}}{\mu}\right) ATP + CH_xO_yN_z + \varepsilon_x CO_2 + (1-\varepsilon_x - y)H_2O + \left(\frac{4.00\,(1+\varepsilon_x) - \gamma_B}{2}\right) NADH_2 = 0 \qquad (R2)$$

The amount of CO_2 produced in the synthesis of 1 C-mol biomass monomer from G6P (ε_x) is 0.131 C-mol. The yield of biomass formation on G6P (α_m) is 0.701 mol ATP/C-mol biomass, calculated from Stouthamer (1973). For polymerization of the biomass precursors (α_x) into new biomass, 1.5 mol ATP/C-mol biomass is required (Verduyn et al., 1991). The term, m_{ATP}, represents the specific ATP consumption due to maintenance. Elemental composition of the biomass without glycogen was found to be $CH_{1.56}O_{0.59}N_{0.19}$ in this study, which gives the degree of reduction (γ_B) of 3.81. When these values are substituted into Reaction (2), the following is obtained:

$$-1.131\mathbf{G6P} - 0.19\,NH_3 - \left(2.201 + \frac{m_{ATP}}{\mu}\right) ATP + CH_{1.56}O_{0.59}N_{0.19} + 0.131\,CO_2 + 0.279\,H_2O + 0.357\,NADH_2 = 0$$

Reaction 3: Primary Carbon Source Catabolism

The catabolism of G6P can be expressed as (Stryer, 1995):

$$-\mathbf{G6P} - H_2O + \frac{5}{6}\,ATP + CO_2 + 2NAPH_2 = 0 \qquad (R3)$$

Reaction 4: Electron Transport Phosphorylation

This reaction describes the oxidation of $NADH_2$, whereby ATP is produced:

$$-NADH_2 - 0.5\,O_2 + H_2O + \delta\,ATP = 0 \qquad (R4)$$

The δ (or the P/O ratio) is the energy efficiency of the reaction (Roels, 1983) and is considered to be independent of the growth rate.

Reaction 5: Synthesis of Storage Polymer Glycogen from G6P

$$-\mathbf{G6P} - \frac{1}{6}\,ATP + \frac{1}{6}\,H_2O + CH_{\frac{10}{6}}O_{\frac{5}{6}} = 0 \qquad (R5)$$

The synthesis of glycogen requires ⅙ ATP per G6P (Stryer, 1995).

Reaction 6: Synthesis of Glucose-6-Phosphate from Glycogen

When the bacterium is deprived of its exogenous source of carbon (glucose), it utilizes glycogen as the energy and carbon source. The phosphorolysis of glycogen into G6P is considered to proceed without consumption of energy (Stryer 1995):

$$-CH_{\frac{10}{6}}O_{\frac{5}{6}} - \frac{1}{6}\,H_2O + \mathbf{G6P} = 0 \qquad (R6)$$

Reaction (R6), in its present form, is a simplification. Glycogen is a branched polymer. The phosphorylase stops cleaving bonds at a distance of 4 glycosyl units from the branching point. Three of the 4 glycosyl units are transferred to another chain by a transferase. At the last glycosyl unit a debranching enzyme must hydrolyze the bond and, as a result, one glucose molecule is released. This unit of glucose will consume 1 mol ATP when phosphorylated into G6P. This ATP consumption is not included in the model because no information on the level of branching of the glycogen is available and also because it has a very marginal effect on net energy consumption. Typically, one in ten residues are branched (Stryer, 1995), leading to a net ATP consumption of 1/60 mol ATP/C-mol glycogen.

In the experiment, the rates of Reactions (R1), (R2), (R4), (R5), (R6), respectively, are measured as:

Substrate uptake rate: $r_1 = -r_s = q_s \cdot C_X$
Biomass formation rate: $r_2 = r_X$
Oxygen uptake rate: $r_4 = -2r_{O_2}$
Glycogen formation rate: $r_5 = r_g^{feast}$
Glycogen degradation rate: $r_6 = r_g^{famine}$

Deduction of Yields and Maintenance Coefficients in Feast Phase

A pseudo-steady state is assumed for the intracellular concentration of ATP, $NADH_2$, and G6P. The net conversion rate of these compounds is therefore equal to zero. Thus, the

following three balances are obtained from Reactions (R1), (R2), (R3), (R4), and (R5). Glycogen degradation (r_6) is considered not to occur when the primary substrate glucose is present (feast phase):

$$\mathrm{NADH_2}: 0 = (2 + 2\varepsilon_X - \frac{1}{2}\gamma_B)\, r_2 + 2r_3 - r_4$$

$$\mathrm{ATP}: 0 = -\frac{1}{6} r_1 - \left(\alpha_m + \alpha_x + \frac{m_{\mathrm{ATP}}}{\mu}\right) r_2 + \frac{5}{6} r_3 + \delta r_4 - \frac{1}{6} r_5$$

$$\mathrm{G6P}: 0 = r_1 - (1 + \varepsilon_X)\, r_2 - r_3 - r_5$$

A balance of the degree of reduction yields:

$$4(-r_s) + (-4)(-r_{O_2}) = 4r_g^{\mathrm{feast}} + \gamma_B r_X$$

These four equations are then substituted, leading to one linear equation for the feast period describing glucose uptake as a function of biomass growth, glycogen production, and maintenance:

$$-r_s = \frac{1}{Y_{sx}^{\max}} r_X + \frac{1}{Y_{sg}^{\max}} r_g^{\mathrm{feast}} + m_s C_X \tag{4}$$

where

$$Y_{sx}^{\max} = \frac{2\delta + \frac{2}{3}}{\frac{1}{2}\gamma_B\delta + \left(\alpha_m + \alpha_x + \frac{5}{6}\varepsilon_X + \frac{5}{6}\right)} \tag{5}$$

$$Y_{sg}^{\max} = \frac{\delta + \frac{1}{3}}{\delta + \frac{1}{2}} \tag{6}$$

$$m_s = \frac{m_{\mathrm{ATP}}}{2\delta + \frac{2}{3}} \tag{7}$$

The values for the metabolic constants from the literature [see description of metabolic Reaction (R2)] and the measured value of the degree of reduction of the biomass (γ_B) are substituted into Eq. (5), which then yields Eq. (8):

$$Y_{sx}^{\max} = \frac{2\delta + \frac{2}{3}}{1.9\delta + 3.14} \tag{8}$$

The r_s and r_x values are estimated from the linear decrease in soluble TOC and ammonium and r_g^{feast} as the linear increase of glycogen in the feast phase.

Deduction of Yield and Maintenance Coefficients in Famine Phase

In the famine phase, it is assumed that the only source of carbon and energy is glycogen. Similar to the derivation just given, the famine phase can be described by using Reactions (R2), (R3), (R4), and (R6). This results in a linear equation [Eq. (9)] for the famine phase, where the consumption of glycogen is a function of the biomass growth and maintenance:

$$-r_g^{\mathrm{famine}} = \frac{1}{Y_{gx}^{\max}} r_X + m_g C_X \tag{9}$$

with the following expressions for the yield factors and the maintenance coefficient:

$$Y_{gx}^{\max} = \frac{2\delta + \frac{5}{6}}{\frac{1}{2}\gamma_B\delta + \left(\alpha_m + \alpha_x + \frac{5}{6}\varepsilon_X + \frac{5}{6}\right)} \tag{10}$$

and:

$$m_g = \frac{m_{\mathrm{ATP}}}{2\delta + \frac{5}{6}} \tag{11}$$

or with the values from the literature and the measured γ_B inserted:

$$Y_{gx}^{\max} = \frac{2\delta + \frac{5}{6}}{1.9\delta + 3.14} \tag{12}$$

The r_g^{famine} and r_x are estimated from the amount of glycogen and ammonium consumed over the famine phase divided by the length of the famine phase (Table II).

KINETIC MODEL

Glycogen is a branched storage polymer, unlike PHB, which is a straight-chain polymer (Dawes and Senior, 1973). The branching is simplified as illustrated in Figure 2.

Stryer (1995) concluded that branching, because it increases the number of terminal points at which the degradation enzymes can attack, will enhance the rate of glycogen synthesis and degradation. This is contradictory to experimental results, which show that faster glycogen consumption corresponds to a lower degree of branching (Zevenhuizen and Ebbink, 1974). The probable reason for

Table II. Duration of the feast and famine phases for the two SRTs and the corresponding concentrations of active biomass.

SRT (days)	C_x (C-mmol/L)	Feast phase (min)	Famine phase (min)
3.6	54	3	237
7.7	99	2	238

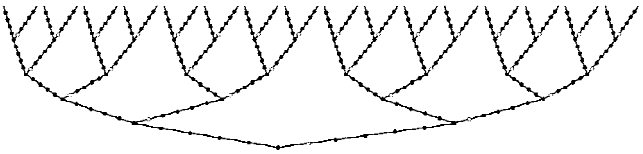

Figure 2. Schematic representation of the branched structure of the proposed model of glycogen. (○) Glycosyl unit linked with a α-1, 6 linkage, which needs to be hydrolyzed; (●) glycosyl unit linked with a α-1,4 linkage, which can be phosphorylated if it is at a distance of at least 4 glycosyl units from a α-1,6 linkage.

this is that the branching also increases the density of glycosyl units in the tiers as the glycogen molecule grows in size. As seen in Figure 2, each time a new tier is completed the volume of the glycosyl chains is doubled, but if a spherical shape is assumed the volume increases by less than a factor two after four tiers. This means that the free space available for the enzymes to attack the bonds is dramatically reduced after four tiers. The consequence of this is that the glycogen molecule is normally assumed to consist of only 12 tiers (Melendez et al., 1997). The tree-like structure also has the effect that the amount of glycosyl units available before action of the debranching enzyme is needed, is around 30% of the total number of units in the glycogen molecule. It must therefore be considered that this outer part of the glycogen molecule is mobilized quite rapidly. These different effects are not easily incorporated into a model, especially if no detailed knowledge of structure (degree of branching) and potential rate-limiting enzymes is available. We therefore attempted to describe the glycogen degradation using a simple empirical multiple-order expression.

In the estimation method corresponding to Eqs. (4) and (9) usually only the start and end values of the feast and famine phases (i.e., the stoichiometric data) are used; see, for instance, Beun et al. (2000a). Because intermediate data are available, a kinetic model is constructed taking the full data set of ammonium and glycogen into account. The kinetic model was implemented in the computer program AQUASIM (Reichert et al., 1998). The removal of glycogen is described by the expression:

$$q_g^{\text{famine,model}} = \frac{df_{\text{gly}}}{dt} = -k \cdot f_{\text{gly}}^{n} \tag{13}$$

In the modeling procedure, it is furthermore assumed that the measured ammonium uptake is a measurement of the growth process on glycogen. The measured uptake of ammonium is therefore coupled with the removal of glycogen in Eq. (14), and by linking Eq. (13) to Eq. (9):

$$r_x = q_g^{\text{famine,model}} \cdot Y_{gx} \tag{14}$$

By fitting the individual curves for the measured ammonium uptake to Eq. (14), one Y_{gx} for each SRT is obtained. Similarly, by fitting all of the ammonium curves to Eq. (9) combined with Eq. (14), $Y_{gx}^{\max}$ and m_g are derived. These four parameter values give two equations (one for each SRT), with two unknowns remaining. The two unknowns are the average growth rates in the famine phase (μ^{famine}) for the two SRTs. When the average growth rate in the famine phase is known, the growth rate during the feast phase can be estimated from the total average growth rate. This is done by subtracting the calculated growth rate in the famine phase from the overall growth rate, taking the time length of the different phases into account.

A potential effect of cell internal metabolites left after the rapid uptake of glucose, which created an ammonium uptake due not only to growth on glycogen, was avoided by excluding the first 20 min of ammonium measurements in the parameter estimation.

RESULTS

General Observations

The SBRs typically reached steady state 3 weeks after inoculation. Steady state was declared when a constant TOC of the suspension in the reactor was obtained and when the cycle profiles of the DO and pH did not change any further. The majority of the sludge settled very fast, but due to microflocs remaining in the supernatant the level of suspended solids in the effluent was relatively high (~30 mg/L). These microflocs could still settle, but not within the 15-min settling period during which the reactor was operated. The settling period was nevertheless not prolonged because of our effort to run the system in a manner as similar as possible to Beun et al. (2000a). The amount of biomass leaving the system with the effluent was taken into account when calculating the SRT. Table II shows the duration of the feast and famine phases for the two SRTs as well as the corresponding concentrations of active biomass.

In Figure 3, the change in cycle concentrations is shown for the SRT of 7.7 days. In Table III, the measured converted amounts of the different compounds are given for the two SRTs. The biomass production is calculated based on the uptake of ammonium. The uptake of glucose in the system was extremely fast. As can be seen in Figure 3a, the majority of the uptake had already occurred when the first DOC sample was taken. When the next sample was taken 5 min later, the substrate was completely removed from the water phase and the concentration of glycogen had started to decrease. The q_s^{feast} and q_g^{feast} were estimated assuming that the removal of glucose and the build-up of glycogen occurred linearly and that the concentration of biomass was constant. The background level of dissolved organic matter (DOC) in the reactor was due to the ethylene-diamine tetraacetic acid (EDTA) present in the nutrient solution.

To validate the rates obtained for the feast phase in the normal cycles (Table IV), experiments with a higher dosage of glucose (approximately tenfold the normal amount) were carried out. The rates obtained in these experiments were comparable to those obtained in the normal cycle measurements.

The maximal formation of PHB was equivalent to 3% (C-mmol/C-mmol) of the dosed glucose. The amount varied

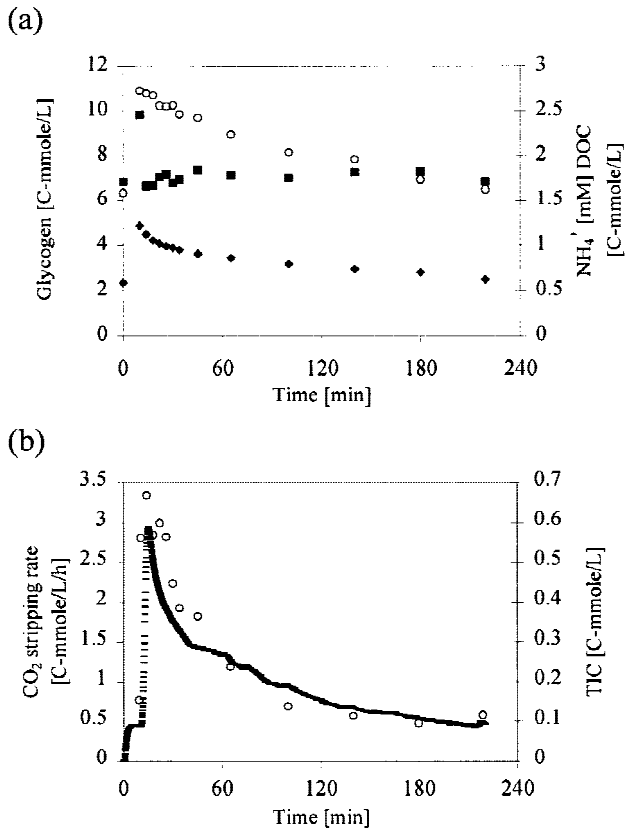

Figure 3. SRT 7.7-day cycle measurement. (a) (○) Glycogen (C-mmol/L), (■) DOC (C-mmol/L), and (♦) NH_4^+ (m*M*). (b) (−) CO_2 stripping rate (C-mmol/L · h) and (○) total inorganic carbon (TIC) (C-mmol/L).

between 0.5% and 3% and f_{PHB} never exceeded 0.004 C-mmol/C-mmol. PHB was therefore not taken into account in the modeling.

Kinetics

The degradation of glycogen was described by multiple-order kinetics [Eq. (13)]. The constant (k) in Eq. (13) was estimated to be 2.6 and the order (n) to be 2 by the least-squares method:

$$q_g^{\text{famine,model}} = \frac{df_{\text{gly}}}{dt} = -2.6 \cdot f_{\text{gly}}^2 \qquad (15)$$

The result of the kinetic modeling of the glycogen degradation is shown in Figure 4.

The results of the estimation of the growth rate are shown in Table V, and yield and maintenance on glycogen are shown in Table VI. In the calculation, it is assumed that glycogen is the only source of carbon in the famine phase.

Table III. Converted amounts of glucose, glycogen, biomass, CO_2 and NH_4^+.

Phase	Compound	Converted amounts (C-mmol/cycle) SRT 3.6 days	SRT 7.7 days
Feast	Glucose dosed	−12.46	−12.44
	Glycogen formed	10.94	9.25
	Biomass formed	*0.68*	*0.30*
	CO_2 formed	*0.84*	*2.89*
	NH_4^+ uptake (N-mmol)	−0.13	−0.06
Famine	Glycogen converted	−10.96	−9.35
	Biomass formed	*5.75*	*4.14*
	CO_2 formed	6.21	5.07
	NH_4^+ uptake (N-mmol)	−1.10	−0.79
Total	*Biomass formed*	*6.43*	*4.44*
	CO_2 formed	7.05	7.96

Biomass formed is calculated based on ammonium uptake. The CO_2 formed in the feast phase is calculated based on C balance. Calculated amounts is given in italics.

Table IV. Values of the various specific rates used in the parameter estimation in the metabolic model.

SRT (days)	$-q_s^{\text{feast}}$ *	q_g^{feast} *	$-q_g^{\text{feast}}/q_s^{\text{feast}}$ †
3.6	2.07	1.81	0.88
7.7	2.02	1.49	0.74

*Data expressed as C-mmol/C-mmol · h. †Data expressed as C-mmol/C-mmol.

Stoichiometry Obtained from Stoichiometric and Kinetic Modeling

Values of δ and m_{ATP} were estimated in two ways, as shown in Table VII. The first was based on the average conversion in the feast and famine phases, giving a δ of 1.8 and m_{ATP} of 0.017. The second approach used a kinetic model and glycogen correlation during the famine phase. This resulted in a δ of 1.4 and an m_{ATP} of 0.012. The δ and m_{ATP} coefficients are strongly coupled and cannot easily be estimated independently. Both parameter sets give practically the same yield coefficients.

In Table VI only the yields obtained from kinetic modeling on the time series of glycogen and ammonium are shown. The yields obtained by the stoichiometric method were not significantly different.

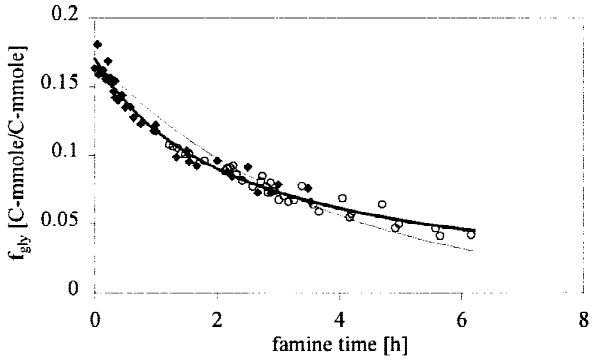

Figure 4. The fraction of glycogen in the famine phase of a cycle in the SBR. (−) Model (the best fit) $q_g^{\text{famine,model}} = df_{\text{gly}}/dt = -2.6 \cdot f_{\text{gly}}^2$; (−) first-order model: $df_{\text{gly}}/dt = -0.28 \cdot f_{\text{gly}}$; (○) f_{gly} from the 7.7-day SRT; (♦) f_{gly} from the 3.6-day SRT.

Table V. Growth rates calculated by metabolic and kinetic modeling in the feast and famine phases and the ratios between them.

SRT (days)	$\mu^{overall}$ (day^{-1})	μ^{feast} (day^{-1})	μ^{famine} (day^{-1})	$\mu^{feast}/\mu^{overall}$ (−)	$\mu^{famine}/\mu^{overall}$ (−)	μ^{feast}/μ^{famine} (−)
3.6	0.278	1.44	0.261	5.2	0.94	5.5
7.7	0.130	0.378	0.128	2.9	0.98	3.0

DISCUSSION

Feast Phase

In the short feast phase, the growth rates are higher than the average growth rate in the famine phase. If the average growth rate is used to model the feast phase (the procedure in ASM3; see Gujer et al. [1999]), the calculated amount of glycogen formed would be overestimated. The growth rates found in the feast phase (Table V) are similar to those found by Beun et al. (2000a).

The overall conclusion concerning the processes occurring in the feast phase is that the physiology is utilized in the form of both a growth and storage response to maximize the substrate uptake. The organisms are probably growing very fast compared with their average growth rate in the system, but due to the very short duration of the feast phase the growth in this phase does not contribute significantly to overall growth.

Comparison Between PHB and Glycogen Storage

In the metabolic model, three macroscopic yields (Y_{sx}, Y_{sg}, and Y_{gx}) and two macroscopic maintenance coefficients (m_s and m_g) are reduced to one microscopic yield (δ) and one microscopic maintenance coefficient (m_{ATP}). This has the clear advantage of reducing the number of free parameters and creating a more consistent description.

To evaluate the differences between glycogen and PHB as storage polymers, the results from the two metabolic models presented in this study and that of Beun et al. (2000a) are compared. In Figure 5, the ratio between the maximum yield of glycogen on glucose (Y_{sg}^{max}) is compared with the maximum yield of PHB on acetate (Y_{sp}^{max}). At $\delta = 1.75$, the Y_{sg}^{max} is 46% larger than Y_{sp}^{max}.

This large difference is due to the fact that storage of glycogen is more efficient than storage of PHB (in terms of spent ATP, 0.17 mol ATP/C-mol G6P relative to 0.25 mol ATP/C-mol acetyl-CoA) and that 1 C-mol of G6P contains more energy than 1 C-mol of acetyl-CoA.

This is even more clearly seen when oxygen consumption due to storage is compared. As shown in Figure 6, the oxygen consumption (OC) when glucose is converted into glycogen is approximately 5% to 10% of the dosed substrate COD, whereas the corresponding OC for the conversion of acetate into PHB is around four times this amount. The maintenance consumption of glycogen was 10% to 15% smaller than maintenance consumption of PHB. This was partly due to the fact that the phosphorolysis of 1 unit of glycogen into the metabolite G6P (r_6) practically runs without ATP consumption, whereas the synthesis of acetyl-CoA from PHB consumes 0.25 mol ATP/C-mol PHB (Van Aalst-van Leeuwen et al., 1997). The smaller maintenance consumption of glycogen is also due to the higher energy content in G6P as compared with acetyl-CoA.

The loss of energy due to the storage into glycogen instead of direct growth can be quantified by calculating the ratio:

$$\frac{(Y_{sx}^{max})_g}{Y_{sx}^{max}} = \frac{Y_{sg}^{max}\, Y_{gx}^{max}}{Y_{sx}^{max}} = \frac{2\delta + \frac{5}{6}}{2\delta + 1}$$

This ratio shows a loss of 4% with a δ of 1.75, demonstrating that the loss of energy due to the incorporation of the storage mechanism in the growth process is quite insignificant. The energy loss in the case of glycogen formation and subsequent consumption is approximately half of the value for PHB (Beun et al., 2000a). Thus, from an energy point of view, storage as glycogen is more favorable than PHB storage. This is also consistent with the experimental results in this research and in the literature (Goel et al., 1998).

Storage Polymer Degradation Kinetics in Famine Phase

The degradation rate of glycogen is well described by second-order kinetics. The reason why a higher reaction order

Table VI. Maximum yield and maintenance coefficients from the kinetic modeling.

Parameter	Value	Dimension
Y_{sx}^{max}	0.60	C-mol/C-mol
Y_{sg}^{max}	0.91	C-mol/C-mol
Y_{gx}^{max}	0.63	C-mol/C-mol
m_s	0.0030	C-mol/C-mol/day
m_g	0.0029	C-mol/C-mol/day

Table VII. Values obtained for δ and m_{ATP} based on stoichiometric and kinetic modeling data from this study and from the literature.

Reference	δ	m_{ATP}	Estimation with
Kinetic modeling	1.4	0.012	Eqs. (9), (13), and (14)
Beun et al. (1999)	1.6	0.015	
Stoichiometric modeling	1.8	0.017	Eqs. (4) and (9)
Smolders et al. (1994)	1.85	0.019	

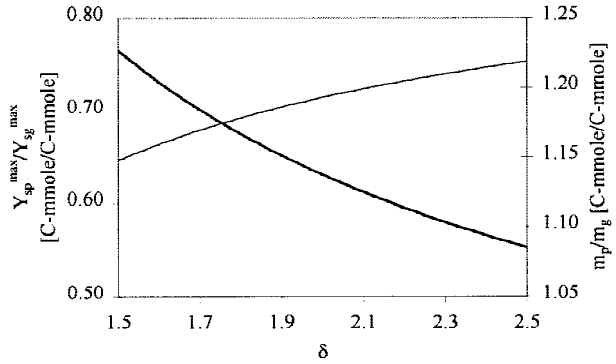

Figure 5. The ratios between $Y_{sp}^{max}/Y_{sg}^{max}$ (–) and m_p/m_g (−). The value of Y_{sp}^{max} calculated as $(4\delta - 2)/(4.5\delta)$, and m_p as $m_{ATP}/(2.25\delta - 0.25)$ (Beun et al., 2000a).

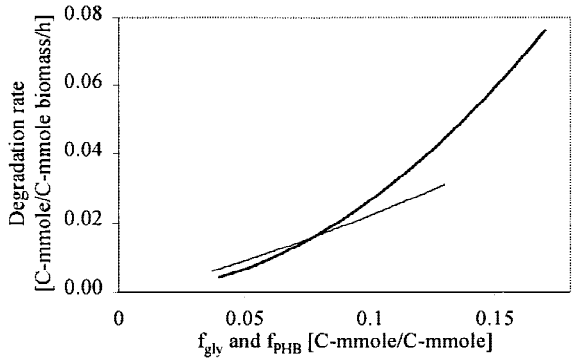

Figure 7. The degradation rate of glycogen, expression $q_g^{famine} = -2.6 \cdot f_{gly}^2$ (-), and PHB (−), expression $q_P^{famine} = -0.44 \cdot f_{PHB}^{1.3}$ (Beun et al., 2000a).

is obtained for glycogen than for PHB ($n = 1.3$) (Beun et al., 2000a) could be that the amount of glycosyl present in the outer layer is directly available for phosphorylation, without action from the other glycogen-degrading enzymes or simply because PHB is linear whereas glycogen is a branched polymer. Thus, an initially high rate is obtained. In Figure 7, the degradation rate of glycogen ($q_g^{famine,model}$) and PHB ($q_p^{famine,model}$) is shown, calculated as $df_{gly}/dt = -2.6 \cdot f_{gly}^2$ and $df_{PHB}/dt = -0.44 \cdot f_{PHB}^{1.3}$, respectively. It shows that the rate of glycogen degradation is faster than that of PHB, as found by Beun et al. (2000a) at the higher fractions (curves intercept at $f = 0.08$ C-mol/C-mol). This is not that surprising because the yield of glycogen on glucose (Y_{sg}) is higher than that of PHB on acetate (Y_{sp}). One would therefore expect that a larger amount of C-moles of glycogen must be converted into biomass over one cycle. If this were not the case, the biomass in this study would leave the system with a larger portion of unutilized storage polymer, as compared with the system of Beun et al. (2000a). The difference in the rates is not due to different yields of biomass on the storage polymer, because the metabolic models (Beun et al. [2000a] and this study) show similar values of Y_{px}^{max} and Y_{gx}^{max}. In studies of metabolism of PHB and glycogen, done simultaneously, it was also shown that, under growth conditions, glycogen is immobilized first and degraded at a faster rate (Zevenhuizen and Ebbink, 1974).

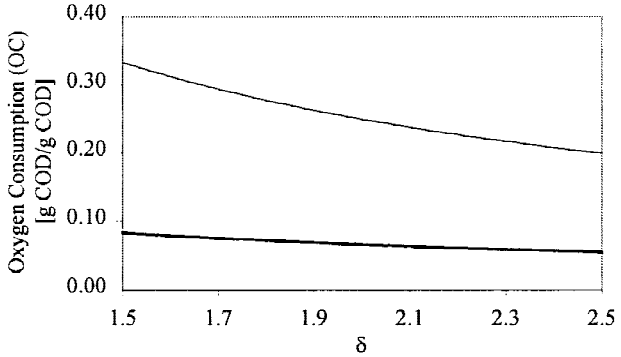

Figure 6. Oxygen consumption (OC) due to storage, calculated as $1 - Y_{sg}^{max}$ for glycogen (−), and as $1 - Y_{sp}^{max}$ for PHB (−).

The $q_g^{famine,model}$ value is smaller than the $q_p^{famine,model}$ value at the lower fractions. This simply illustrates that the m_g is lower than m_p, because, at these low levels of storage polymer, the glycogen (or PHB) is used predominately for maintenance. This is also indicated by the fact that the rate for PHB degradation is 0.006 C-mol/C-mol/h ($m_P = 0.0044$) and for glycogen 0.004 C-mol/C-mol · h ($m_g = 0.004$) at the lowest fractions examined. These rates are very close to the corresponding maintenance coefficients.

Implementation of Storage of Glycogen and PHB in ASMs

The yield coefficients in ASMs are generally based on a black-box approach. If the information from the different metabolic pathways is included in the models, the relation between the yields becomes obvious and will lower the number of stoichiometric coefficients needed (e.g., Beun et al., 2000a; Smolders et al., 1994). Because the reported values of δ and m_{ATP} (Table VII) are not significantly different, it is possible that not all yield values for different processes could be coupled to one δ value.

The results of the metabolic modeling in this study, and those of Beun et al. (2000a), have clearly shown that there are significant differences in the yield of storage polymer (PHB and glycogen) on the substrate. In ASM3, an average storage yield is used to describe the oxygen consumption (OC) due to storage of municipal wastewater. Figure 6 clearly demonstrates that the OC is very dependent on the distribution between VFA and carbohydrates in the wastewater. Because ASM3 does not distinguish between various COD components with respect to yield this could lead to an inexact estimation of the OC, especially if the distribution between VFA and carbohydrate in the wastewater COD changes over the period that an investigator intends to model.

In ASMs, the most common way to express the kinetics of microbial conversions is via Monod kinetics (Gujer et al., 1999):

$$\frac{df_{STO}}{dt} = -\frac{\mu_H}{Y_{max}} \frac{f_{STO}}{K_{STO} + f_{STO}} \tag{16}$$

The typical value of the half-saturation constant (K_{STO}) in ASM3 is 1 g COD/g COD (Gujer et al., 1999). Using this value, the Monod term will resemble first-order kinetics, because the f_{STO} in question is typically much lower than 1 g COD/g COD. The same phenomenon is observed when fitting the f_{gly} data to Eq. (16). The fit simply gets better as the value of K_{STO} is increased, while keeping the ratio between (μ_H/Y_{max}) and K_{STO} at 0.28. Under these conditions, the Monod term is similar to first-order kinetics with a k value of 0.28. First-order kinetics clearly fails to provide a good fit of the data (Fig. 4). Although the second-order expression provides a nice fit with the data obtained, this does not necessarily mean that such an approach should be chosen in future ASMs. In ASM3, the Monod term [Eq. (16)] is used to model the sum of all stored material. Its function is therefore not solely to describe the degradation of glycogen. However, Beun et al. (2000a) also found an order higher than one ($n = 1.3$) for the degradation of PHB. A clearer understanding of the different mechanisms behind the degradation of storage polymers would be very useful for obtaining a more exact kinetic expression, or at least a clearer understanding of the limitations of the presently used models. The complexity of a future ASM would of course be increased, because stored material would at least have to be divided into a glycogen and a PHA fraction. This would affect the wastewater characterization. It should include a division of the COD into a COD suitable for either glycogen or PHA production. This would be different from the present wastewater characterization, which describes mainly the degree of biodegradability of the COD. It would be of interest to see if a more detailed chemical wastewater characterization (e.g., VFA, carbohydrate, protein, and lipid content) would yield more valuable data for modeling. In applying ASM3, one should pay attention to which polymers could be formed from the compounds in the wastewater, and adjust the model constants correspondingly. The identification and role of storage compounds other than glycogen and PHA in the activated sludge processes remains as an important topic for future research.

CONCLUSIONS

- Storage of glucose as glycogen is a mechanism used under dynamic conditions to balance the growth process.
- The storage of glycogen and subsequent growth can occur without significant loss of energy, as compared with direct growth on glucose (only 2% to 6% lower biomass yield).
- Glycogen is formed faster and is utilized faster (C-mol/C-mol biomass/h) than PHB at the same level of storage (C-mol polymer/C-mol biomass/h).
- The yield of biomass on the storage polymer is similar for glycogen and PHB (C-mol/C-mol).
- The energy needed for maintenance (ATP) is the same for glycogen and PHB; however, in C-mol/C-mol maintenance on glycogen, it is 10% to 15% lower than that of PHB.

The authors thank the staff at the Kluyver Laboratory for Biotechnology, Technical University of Delft, for the analytical work performed.

NOMENCLATURE

ASM	activated sludge model
C_X	active biomass concentration (C-mmol/L)
DO	dissolved oxygen (%)
DOC	dissolved organic carbon
f_{gly}	fraction of glycogen of the total active biomass (C-mol/C-mol)
f_{STO}	fraction of stored COD in ASM3 (COD/COD)
G6P	glucose-6-phosphate
GLY	glycogen
k	reaction rate constant
K_{STO}	saturation constant for stored COD in ASM3 (COD/COD)
m_{ATP}	maintenance coefficient based on ATP (mol/C per mol · h)
m_g	maintenance coefficient for growth on glycogen (C-mol/C-mol · h)
m_p	maintenance coefficient for growth on PHB (C-mol/C-mol · h)
m_s	maintenance coefficient for growth on glucose (C-mol/C-mol · h)
Mw (X)	molecular weight of biomass (g/C-mol)
Mw (GLY)	molecular weight of glycogen = 27 g/C-mol
Mw (PHB)	molecular weight of PHB = 21.5 g/C-mol
n	reaction order (-)
OC	oxygen consumption
PHA	polyhydroxyalkanoates
PHB	poly-β-hydroxybutyrate
$-q_{O2}$	specific oxygen consumption rate (O_2-mol/C-mol · h)
$-q_g$	specific glycogen consumption rate (C-mol/C-mol · h)
q_g^{feast}	specific GLY production rate in the feast phase (C-mol/C-mol · h)
$-q_s^{feast}$	specific glucose uptake rate in the feast phase (C-mol/C-mol · h)
$-q_g^{max}$	maximum specific glucose uptake rate (C-mol/C-mol · h)
$q_g^{famine,model}$	specific glycogen consumption rate in the famine phase calculated from the model expression (C-mole/C-mol · h)
$q_p^{famine,model}$	specific PHB consumption rate calculated from the model expression (C-mol/C-mol · h)
r_g^{feast}	glycogen production rate in the feast phase (C-mmol/L · h)
r_g^{famine}	glycogen consumption rate in the famine phase (C-mmol/L · h)
$-r_s$	glucose uptake rate (C-mmol/L · h)
r_x	biomass growth rate (C-mmol/L · h)
SBR	sequencing batch reactor
SRT	sludge retention time (days)
t	time (h)
V	volume (L)
Y_{gx}	yield of biomass on glycogen (C-mol/C-mol)
Y_{gx}^{max}	maximum yield of biomass on glycogen (C-mol/C-mol)
Y_{px}^{max}	maximum yield of biomass on PHB (C-mol/C-mol)
Y_{sg}^{max}	maximum yield of glycogen on glucose (C-mol/C-mol)
Y_{sx}^{max}	maximum yield of biomass on glucose (C-mol/C-mol)
$(Y_{sx}^{max})_g$	maximum yield of biomass when the primary substrate glucose is first transformed into glycogen (C-mol/C-mol)

Greek symbols

δ	$P/2e^-$ ratio = ATP produced per $NADH_2$ oxidized (mol/mol)

γ_B	degree of reduction of the biomass
μ^{feast}	specific growth rate in feast phase (h^{-1})
μ^{famine}	specific growth rate in famine phase (h^{-1})
$\mu^{overall}$	average specific growth rate over one cycle (h^{-1})

References

Beun JJ, Paletta F, Van Loosdrecht MCM, Heijnen JJ. 2000a. Stoichiometry and kinetics of poly-β-hydroxybutyrate metabolism in aerobic, slow growing, activated sludge cultures. Biotechnol Bioeng 67: 379–389.

Beun JJ, Verhoef EV, Van Loosdrecht MCM, Heijnen JJ. 2000b. Stoichiometry and kinetics of poly-β-hydroxybutyrate metabolism under denitrifying conditions in activated sludge cultures. Biotechnol Bioeng (in press).

Cech JS, Chudoba J. 1983. Influence of accumulation capacity of activated sludge microorganisms on kinetics of glucose removal. Water Res 7:361–374.

Dawes EA, Senior PJ. 1973. The role and regulation of energy reserve polymers in micro-organisms. In: Rose AH, Tempest DW, editors. Advances in microbial physiology. London: Academic Press. p 136–266.

Dircks K, Pind PF, Mosbæk H, Henze M. 1999. Yield determination by respirometry—the possible influence of storage under aerobic conditions in activated sludge. Water SA 25:69–74.

Goel R, Mino T, Satoh H, Matsuo T. 1998. Intracellular storage compounds, oxygen uptake rates and biomass yield with readily and slowly degradable substrates. Water Sci Technol 38:85–93.

Gujer W, Henze M, Takashi M, Van Loosdrecht MCM. 1999. Activated sludge model no. 3. Water Sci Technol 39:183–193.

Krishna C, Van Loosdrecht MCM. 1999. Substrate flux into storage and growth in relation to activated sludge modeling. Water Res 33: 3149–3161.

Melendez R, MelendezHevia E, Cascante M 1997. How did glycogen structure evolve to satisfy the requirement for rapid mobilization of glucose? A problem of physical constraints in structure building. J Mol Evol 45:446–455.

NNI. 1982. NEN 6621. Bepaling van de asrest. Delft: Nederlands Normalisatie Instituut.

Reichert P, Ruchti J, Simon W. 1998. AQUASIM 2.0 delta. Duebendorf, Switzerland: Swiss Federal Institute for Environmental Science and Technology (EAWAG). 213 p.

Roels JA. 1983. Energetics and kinetics in biotechnology. Amsterdam: Elsevier. 330 p.

Smolders GJF, Van der Meij J, Van Loosdrecht MCM, Heijnen JJ. 1994. Stoichiometric model of the aerobic metabolism of the biological phosphorus removal process. Biotechnol Bioeng 44: 837–848.

Stainer RY, Doudoroff M, Kunisawa R, Contopoulou R 1959. The role of organic substrates in bacterial photosynthesis. Proc Natl Acad Sci USA 45:1246–1260.

Stouthamer AH. 1973. A theoretical study on the amount of ATP required for synthesis of microbial cell material. Antonie van Leeuwenhoek 39:545–565.

Stryer L. 1995. Biochemistry. New York: WH Freeman and Co. 1064 p.

Van Loosdrecht MCM, Pot MA, Heijnen JJ. 1997. Importance of bacterial storage polymers in bioprocesses. Water Sci Technol 35:41–47.

Van Aalst-van Leeuwen MA, Pot MA, Van Loosdrecht MCM, Heijnen JJ. 1997. Kinetic modeling of poly(β-hydroxybutyrate) production and consumption by *Paracoccus pantotrophus* under dynamic substrate supply. Biotechnol Bioeng 55:773–782.

Verduyn C, Stouthamer AH, Scheffers WA, Van Dijken JP. 1991. A theoretical evaluation of growth yields of yeasts. Antonie van Leeuwenhoek 59:49–63.

Vishniac W, Santer M. 1975. The *Thiobacilli*. Bacteriol Rev 21:195–213.

Wilkinson JF. 1959. The problem of energy-storage compounds in bacteria. Exp Cell Res 7(suppl):111–130.

Zevenhuizen LPTM, Ebbink AG. 1974. Interrelations between glycogen, poly-β- hydroxybutyric acid and lipids during accumulation and subsequent utilization in a *Pseudomonas*. Antonie van Leeuwenhoek 40: 103–120.